Journal of Materials Chemistry B

COMMUNICATION

View Article Online
View Journal | View Issue

Cite this: J. Mater. Chem. B, 2015, 3, 1470

Received 11th December 2014
Accepted 6th January 2015

DOI: 10.1039/c4tb02036g

www.rsc.org/MaterialsB

Multivalent manganese complex decorated amphiphilic dextran micelles as sensitive MRI probes†

Changqiang Wu,‡[a] Danyang Li,‡[ab] Li Yang,[a] Bingbing Lin,[a] Houbing Zhang,[a] Ye Xu,[a] Zhuzhong Cheng,[a] Chunchao Xia,[c] Qiyong Gong,[c] Bin Song[c] and Hua Ai*[ac]

T_1 contrast agents based on Mn(II) were conjugated on amphiphilic dextran micelles *via* click chemistry. The obtained paramagnetic nanomicelle contrast agent has a higher T_1 relaxivity (13.3 Mn mmol^{-1} s^{-1}) and better sensitivity than those of free Mn(II) complexes. Studies carried out *in vivo* suggest that this contrast agent has a better and long-acting vascular enhancement effect at a lower manganese dosage (0.1 Mn mmol kg^{-1} BW).

Magnetic resonance imaging (MRI) contrast agents play important roles in disease diagnosis and therapeutic efficacy evaluation. Paramagnetic metal ions (manganese(II), iron(III) and gadolinium(III)) have the ability to shorten the longitudinal relaxation time (T_1) of water protons, and can be used as MRI contrast agents in biomedical research and early diagnosis of diseases. Particularly, complexes based on gadolinium(III) have been widely studied in the past few years,[1–6] and are the major choices of clinical MRI contrast agents (Magnevist®, Omniscan®, OptiMARK™ and MultiHance™ *etc.*), because of their high spin and slow electronic relaxation. However, the clinical use of gadolinium-based contrast agents is conditionally restricted by the Food and Drug Administration (FDA), due to the side effects that cause nephrogenic systemic fibrosis (NSF) in patients with reduced kidney function.[7–9] Compared with other paramagnetic metal ions, manganese(II) can be an appropriate alternative to gadolinium(III) due to several advantages. Specifically, manganese is a biogenic element (0.5–1.2 μg L^{-1} in serum), and also a cofactor in a number of critical biological enzymes. It has slow electronic relaxation (10^{-8} to 10^{-9} s) and high spin with five unpaired electrons in the outermost electron orbit.

Manganese(II) has been used as a contrast agent in MRI studies for many years.[10–13] However, the relaxivity and stability of manganese complexes are inferior to that of the gadolinium complex due to its physical properties and large doses of manganese(II) ions are neurotoxic despite their important biological role.[14] Therefore, our work focuses on increasing the sensitivity of manganese contrast agents and reducing metal ion dosages. In our previous work,[15] a manganese–ligand (MnL) based T_1 contrast agent was successfully developed and its T_1 relaxivity is 3.6 Mn mmol^{-1} s^{-1} (1.5 T, room temperature), which is higher than that of a commercialized T_1 contrast agent, Teslascan, also called MnDPDP (2.2 Mn mmol^{-1} s^{-1}, 1.5 T, 20 °C).[16]

In clinical magnetic fields (0.5–3.0 T), one of the most important influencing factors of T_1 relaxivity is the rotational correlation time (τ_R).[1] According to previous reports,[2,17,18] prolonged τ_R by increasing the molecular weight of contrast agents or connecting low molecular weight contrast agents on macromolecules can result in higher T_1 relaxivity. In this work, we chose dextran based amphiphilic polymers as the basic macromolecular building blocks, which can self-assemble into nanomicelles in aqueous solution (Fig. 1). Polysaccharide dextran was chosen as the hydrophilic part because of the following advantages: first, dextran is an excellent biocompatible polymer, and has been used as a plasma substitute or in MRI contrast agent formulations, such as Feridex and Resovist. Second, it has a rigid structure which is beneficial to prolong the τ_R of small molecules conjugated on its side groups. Third, it has been shown that amphiphilic dextran can form stable nanomicelles in a physiological environment, meeting the important requirement for clinical applications.[19,20]

Amphiphilic dextran with azide groups was obtained with three step modifications of dextran (Scheme S1†). Dextran (M_w: 10 kDa) with tosylate groups (Dex-*g*-Ts) grafting on the backbone was obtained by a reaction between TsCl and the hydoxy

[a]National Engineering Research Center for Biomaterials, Sichuan University, Chengdu 610064, P. R. China. E-mail: huaai@scu.edu.cn; Fax: +86-28-85413991; Tel: +86-28-85413991

[b]School of Engineering and Materials Science, Queen Mary, University of London, Mile End Road, London, E1 4NS, UK

[c]Department of Radiology, West China Hospital, Sichuan University, Chengdu 610041, P. R. China

† Electronic supplementary information (ESI) available: Experimental details, spectral characterisation, and analytical data of reported compounds. See DOI: 10.1039/c4tb02036g

‡ These authors contributed equally to this work.

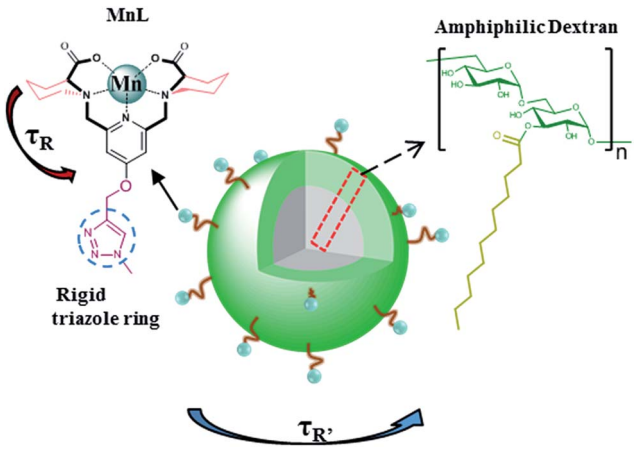

Fig. 1 Manganese complexes were conjugated on the surface of an amphiphilic dextran micelle *via* click chemistry to prolong the rotational correlation time (τ_R). According to the Bloembergen–Solomon–Morgan theory, relaxation rates of contrast agents can be obtained upon an increase of τ_R, which is related to the structures of the carrier and linker.

group (–OH) of dextran. Further modification was carried out to obtain azide group functionalized dextran (Dex-*g*-N_3). The grafting ratio of Ts was 0.38 Ts per sugar unit, initially estimated by the integral area ratio of characteristic peaks in the ^{1}H NMR spectrum. After the azide substitution reaction, characteristic peaks of the tosyl group decreased, with a conversion yield of 29%. Fourier transform infrared spectroscopy (FTIR) characterization was used to confirm that azide groups are successfully introduced into amphiphilic dextran by the appearance of the azide peak (2100 cm^{-1}) (Fig. S3†). In preliminary studies, we also have tried other ways to modify dextran with azide groups (listed in the ESI†). The results show that the reaction efficiency based on the epichlorohydrin ring opening method in the aqueous phase is much lower than that of Ts modification (Fig. S4†). Then, dextran with the azide group grafted with lauric acid (LA) (Dex-*g*-LA/N_3) was synthesized by the esterification reaction between the hydroxyl group (–OH) of Dex-*g*-N_3 and the carboxyl group (–COOH) of LA. LA was chosen as the hydrophobic component and can be observed by ^{1}H NMR of amphiphilic dextran (Fig. S5†).

The grafting ratio of the hydrophobic chain on the hydrophilic polymer backbone, environmental pH and ionic concentration are all important factors related to the micelle stability. The stability is usually estimated by the critical micelle concentration (CMC) and a lower CMC is considered more stable in water. In this work, we found that the grafting ratio of LA on the dextran backbone can be controlled in a time-dependent manner. We stopped the reaction at different time points (3 to 48 hours) and the grafting ratio of LA increased linearly from 0.017 to 0.37 LA per sugar unit (Fig. S6†). It allowed us to precisely control the grafting ratio of the hydrophobic component and to find a formulation with better stability. Next, we chose a LA grafting ratio of 0.29 LA per sugar unit with a CMC of 1.2 mg L^{-1} for micelle formulation because of the good stability and size control (Fig. S7†).

An aza-semi-crown pentadentate ligand with an alkynyl group (l-alkynyl) was synthesized *via* multistep reactions. The synthetic route (Scheme S2†) is similar to that of a previous report,[15] except that the alkynyl group was linked with a pyridine ring of 2,6-bis(chloromethyl)pyridine in advance. The products of each step reaction were characterized by ^{1}H NMR, ^{13}C NMR and mass spectrum, respectively (listed in the ESI†).

Then, Cu(I)-catalyzed azide-alkyne cycloadditions were carried out in a water/dimethylformamide mixture at 60 °C for 48 hours. Afterwards, the copper ion-complexing ligand *N*,*N*,*N*′,*N*′,*N*″-pentamethyldiethylenetriamine (5 eq. to the copper ion) was dissolved in the reaction mixture and stirred for 24 hours. The expected product was collected after the resulting solution was dialyzed for 3 days against water (MWCO 10 kDa cutoff) and then lyophilized. Characteristic peaks of the ligand and Dex-*g*-LA appeared in the ^{1}H NMR spectrum of the end-product (Fig. 2, Dex-*g*-LA/L).

Dex-*g*-LA/L micelles in aqueous solution were prepared by an emulsion and solvent evaporation method,[20] and followed by chelation of manganese(II) to obtain the designed Dex-*g*-LA/MnL nanomicelle solution. Fig. 3a shows that the nanomicelles have a relatively narrow size distribution in water, and have a mean diameter of 85 ± 20 nm characterized by dynamic light

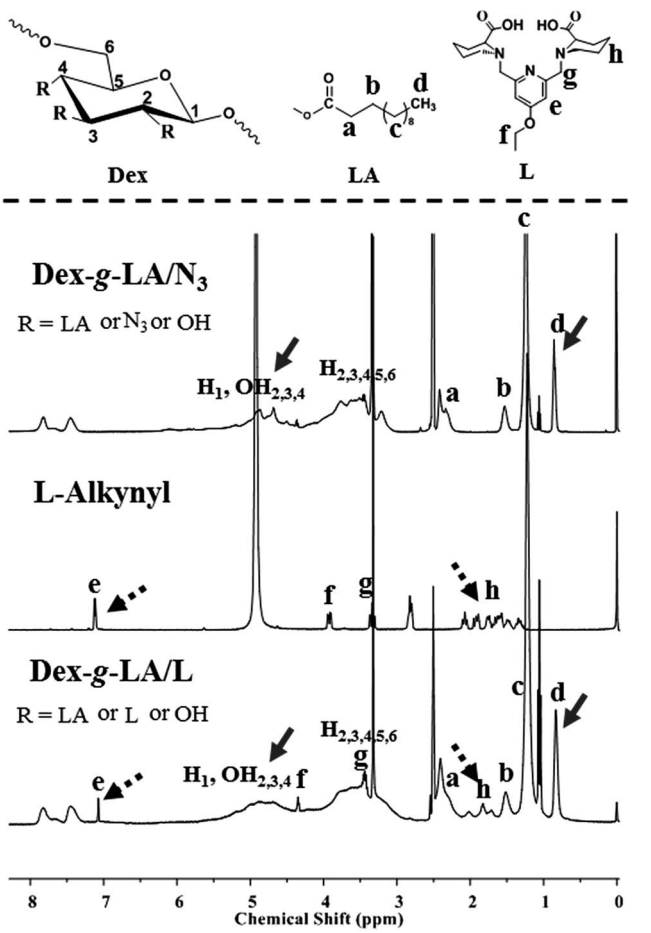

Fig. 2 ^{1}H NMR spectrum of Dex-*g*-LA/N_3 (DMSO), l-alkynyl (D_2O) and Dex-*g*-LA/L (DMSO). Characteristic peaks are identified by regular (Dex-*g*-LA/N_3) and dotted (L) arrows.

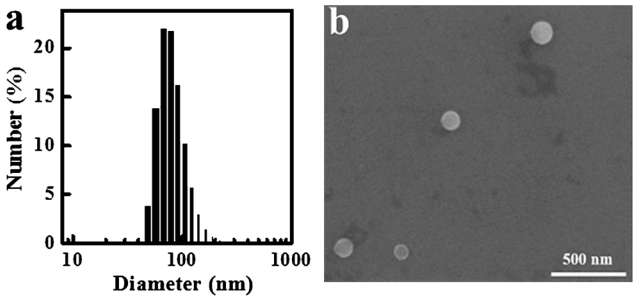

Fig. 3 DLS (a) and SEM (b) of Dex-*g*-LA/MnL nanomicelles. These nanoparticles show a diameter of 85 ± 20 nm in DLS, and a regular spherical structure under a SEM.

scattering (DLS). Amphiphilic dextran nanoparticles with a regular spherical structure are finely disseminated on the silicon wafer under scanning electron microscope (SEM) observation, with a diameter around 100 nm (Fig. 3b).

The T_1 relaxivity of Dex-*g*-LA/MnL nanomicelles and free MnL was measured at 1.5 T on a clinical MR scanner at room temperature. Fig. 4a presents the relaxation rates ($1/T_1$) of samples in aqueous solution at different manganese concentrations. The T_1 relaxivity of Dex-*g*-LA/MnL is 13.3 Mn mmol^{-1} s^{-1} and is about 2.8 times to that of free MnL (4.8 Mn mmol^{-1} s^{-1}). This significant increase in the relaxivity is mainly attributed to the structure of the amphiphilic dextran micelle. First, the stability of the nanostructure provided the contrast agent with a stationary platform, which has a longer rotational correlation time ($\tau_{R'}$) itself and restrains the stochastic motion of the contrast agent to some degree. Moreover, the rigid triazole ring connecting the rigid six-member ring of glucose with manganese(II) complexes is quite important due to its ability to hinder the local rotation of Mn(II) complexes.[21–23] All these factors lead to a prolonged τ_R, and subsequently enhance the relaxivity. It suggests that the T_1 relaxivity of the paramagnetic nanocomposites are improved by decorating MnL on a rigid nanomicelle surface *via* a rigid linker.

At the same time, from the T_1-weighted MRI images (Fig. 4b), we can see that Dex-*g*-LA/MnL nanomicelles have higher MRI signal intensities than free MnL under the same Mn concentration. Dex-*g*-LA/MnL nanomicelles can generate good contrast at a much lower Mn concentration.

T_1 contrast agents can enhance the image contrast of tissue through substantial shortening of T_1 relaxation times and result in hyperintense signals at locations where the probes accumulate. Contrast enhanced magnetic resonance

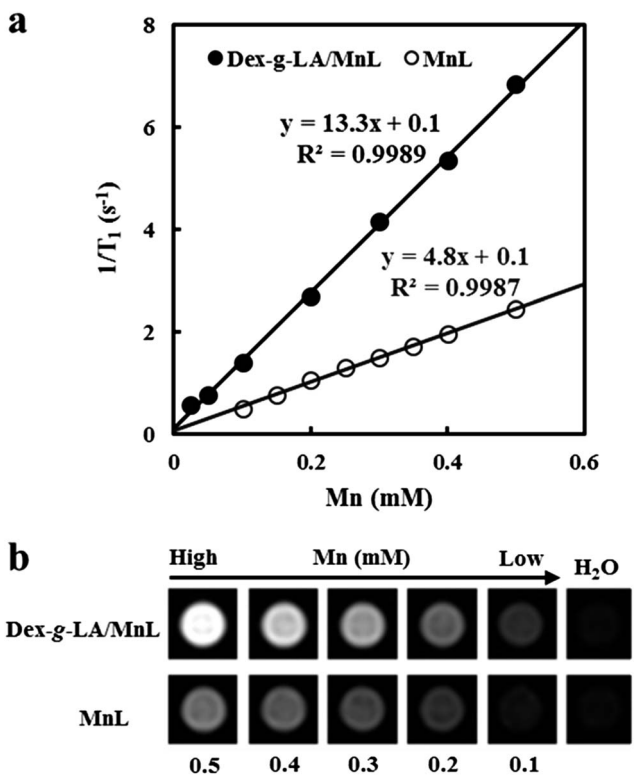

Fig. 4 T_1 relaxivity (a) and T_1-weighted MRI images (b) of Dex-*g*-LA/MnL nanomicelles and free MnL (1.5 T, room temperature). Dex-*g*-LA/MnL nanomicelles have a relaxivity of 13.3 Mn mmol^{-1} s^{-1}, and present higher MR signal intensities than free MnL at the same Mn concentration.

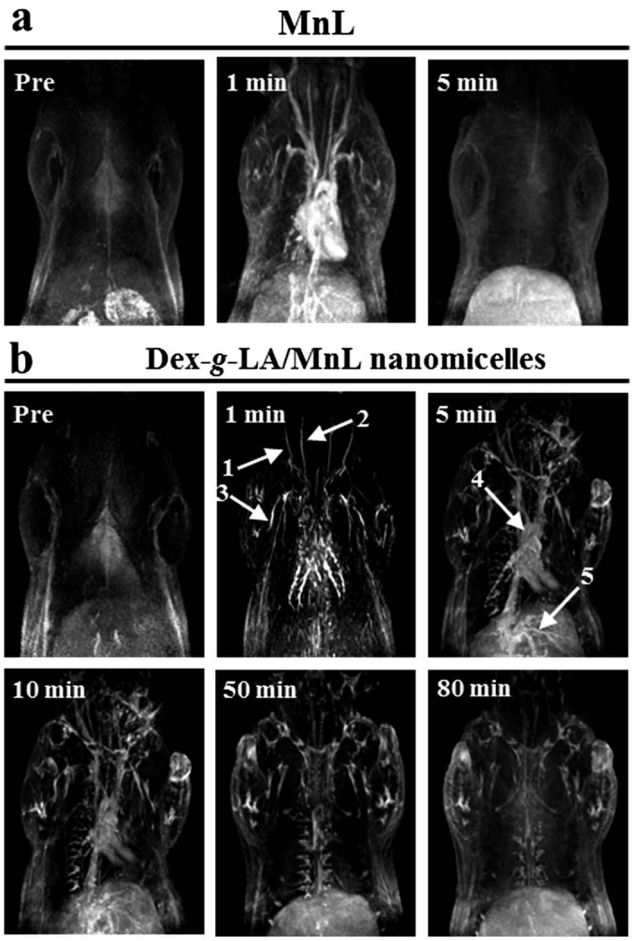

Fig. 5 Contrast enhanced MRA study of SD rats on a clinical 3.0 T scanner. Dosage: 0.1 Mn mmol kg^{-1} BW of MnL (a) and Dex-*g*-LA/MnL nanomicelles (b). Dex-*g*-LA/MnL nanomicelles show a longer vascular enhancement time than free MnL at a lower manganese dosage. Vascular details including: jugular vein (1), carotid artery (2), subclavian vein (3), aortic arch (4), and hepatic portal vein (5).

angiography (MRA) is an imaging technique that uses T_1 contrast agents to shorten T_1 times of blood and to obtain bright images of blood vessels by a T_1-weighted imaging (T_1WI) sequence. Herein, to evaluate Dex-*g*-LA/MnL nanomicelles as a T_1 MRI contrast agent, a contrast enhanced MRA study of SD rats was carried out on a clinical 3 T MR scanner. All studies involving animals were approved by the Animal Care and Use Committee of the Institute. Blood vessel images of the chest and neck regions of rats were obtained after intravenous injection of Dex-*g*-LA/MnL nanomicelles or free MnL at a dosage of 0.1 Mn mmol per kg body weight (Fig. 5). At one min after adminstration of free MnL, the jugular vein, subclavian vein, and aortic arch were clearly visible, but the imaging window was less than five minutes. The major reason is that low molecular weight contrast agents are very quickly cleared through the kidneys. In comparison, Dex-*g*-LA/MnL nanomicelles present a much longer vascular imaging window. As shown in Fig. 5b, vessel signal intensities are significantly enhanced (hepatic portal vein was also clearly visible), and the imaging window maintained up to 50 min at a relatively low manganese dosage compared to clinical dosage. The results show that Dex-*g*-LA/MnL nanomicelles have a long circulation time, probably are slowly phagocytized by the reticuloendothelial system (RES) instead of discharging through the kidneys.

Conclusions

In summary, we designed and synthesized a paramagnetic nanocomposite probe based on manganese(II) complexes (MnL). Multivalent manganese complexes were introduced on amphiphilic dextran micelles by click chemistry. The results indicated that this probe has a much higher T_1 relaxivity (13.3 Mn $mmol^{-1}$ s^{-1}) compared to the free MnL (4.8 Mn $mmol^{-1}$ s^{-1}). In rat MRA, Dex-*g*-LA/MnL nanomicelles presented a better and long-acting vascular enhancement effect at a manganese dosage of 0.1 Mn mmol kg^{-1} BW, which is much lower than many reported studies.

Author contributions

H. Ai conceived and designed the experiments; D. Li and L. Yang performed the synthesis of amphiphilic dextran; C. Wu, B. Lin and H. Zhang performed the synthesis of the ligand with the alkynyl group; C. Xia, Y. Xu and Z. Cheng performed the MRI experiment; B. Song and Q. Gong provided guidance and advice in MRI; H. Ai, C. Wu and D. Li co-wrote the paper. All authors discussed the results and commented on the manuscript.

Acknowledgements

This work was supported by the National Key Basic Research Program of China (2013CB933903), National Key Technology R&D Program (2012BAI23B08), National Natural Science Foundation of China (20974065, 51173117 and 50830107), Program for Changjiang Scholars and Innovative Research Team in University (PCSIRT, Grant no. IRT1272) of China.

Notes and references

1 P. Hermann, J. Kotek, V. Kubicek and I. Lukes, *Dalton Trans.*, 2008, 3027.
2 S. Aime, M. Botta, M. Fasano and E. Terreno, *Chem. Soc. Rev.*, 1998, **27**, 19.
3 P. Caravan, J. J. Ellison, T. J. McMurry and R. B. Lauffer, *Chem. Rev.*, 1999, **99**, 2293.
4 H. Weinmann, R. Brasch, W. Press and G. Wesbey, *Am. J. Roentgenol.*, 1984, **142**, 619.
5 Z. Liu, K. Dong, J. Liu, X. Han, J. Ren and X. Qu, *Small*, 2014, **10**, 2429.
6 Z. Liu, F. Pu, S. Huang, Q. Yuan, J. Ren and X. Qu, *Biomaterials*, 2013, **34**, 1712.
7 P. Marckmann, L. Skov, K. Rossen, A. Dupont, M. B. Damholt, J. G. Heaf and H. S. Thomsen, *J. Am. Soc. Nephrol.*, 2006, **17**, 2359.
8 M. A. Sieber, T. Steger-Hartmann, P. Lengsfeld and H. Pietsch, *J. Magn. Reson. Imaging*, 2009, **30**, 1268.
9 M. R. Prince, H. L. Zhang, J. C. Prowda, M. E. Grossman and D. N. Silvers, *RadioGraphics*, 2009, **29**, 1565.
10 D. Pan, S. D. Caruthers, A. Senpan, A. H. Schmieder, S. A. Wickline and G. M. Lanza, *Wiley Interdiscip. Rev.: Nanomed. Nanobiotechnol.*, 2011, **3**, 162.
11 A. P. Koretsky and A. C. Silva, *NMR Biomed.*, 2004, **17**, 527.
12 M. Thuen, M. Berry, T. B. Pedersen, P. E. Goa, M. Summerfield, O. Haraldseth, A. Sandvig and C. Brekken, *J. Magn. Reson. Imaging*, 2008, **28**, 855.
13 K. Dong, Z. Liu, J. Liu, S. Huang, Z. Li, Q. Yuan, J. Ren and X. Qu, *Nanoscale*, 2014, **6**, 2211.
14 A. Mohadesi and M. Falahnejad, *TheScientificWorldJournal*, 2012, **2012**, 987645.
15 H. Su, C. Wu, J. Zhu, T. Miao, D. Wang, C. Xia, X. Zhao, Q. Gong, B. Song and H. Ai, *Dalton Trans.*, 2012, **41**, 14480.
16 E. Wiener, K. Woertler, G. Weirich, E. J. Rummeny and M. Settles, *Eur. J. Radiol.*, 2007, **63**, 110.
17 H. Ai, *Adv. Drug Delivery Rev.*, 2011, **63**, 772.
18 L. O. Liepold, M. J. Abedin, E. D. Buckhouse, J. A. Frank, M. J. Young and T. Douglas, *Nano Lett.*, 2009, **9**, 4520.
19 Q. Wang, H. Su, C. Xia, J. Sun, C. Liu, Z. Wang, Q. Gong, B. Song, F. Gao, H. Ai and Z. Gu, *Chin. Sci. Bull.*, 2009, **54**, 2925.
20 H. Su, Y. Liu, D. Wang, C. Wu, C. Xia, Q. Gong, B. Song and H. Ai, *Biomaterials*, 2013, **34**, 1193.
21 Z. Zhang, M. T. Greenfield, M. Spiller, T. J. McMurry, R. B. Lauffer and P. Caravan, *Angew. Chem., Int. Ed.*, 2005, **44**, 6766.
22 F. Kielar, L. Tei, E. Terreno and M. Botta, *J. Am. Chem. Soc.*, 2010, **132**, 7836.
23 Y. Song, E. K. Kohlmeir and T. J. Meade, *J. Am. Chem. Soc.*, 2008, **130**, 6662.